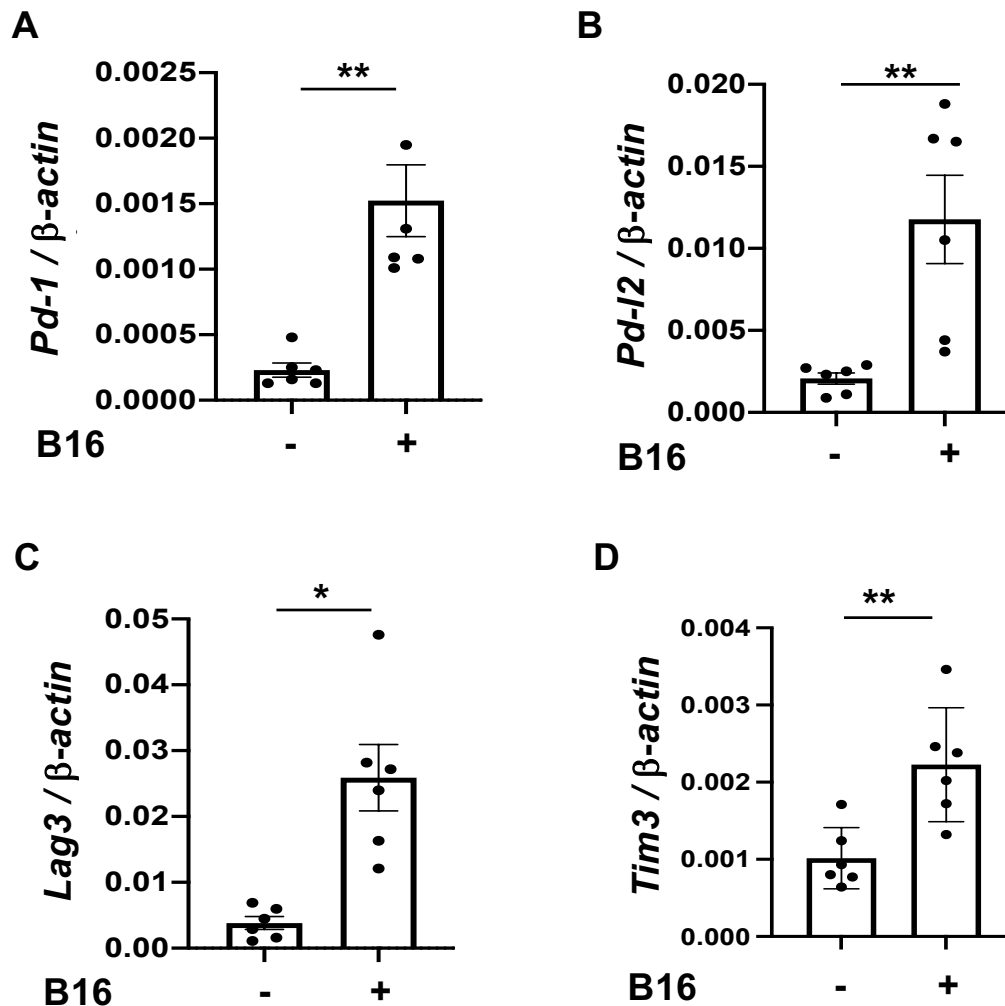


## Supplementary Table

Table S1. Sequences of RT-PCR primers used in this study

Gene	Sequence (5'to 3')	Length
<i>Pd-1-S</i>	ACCCTGGTCATTCACCTTGGG	20
<i>Pd-1-AS</i>	CATTTGCTCCCTCTGACACTG	21
<i>Pd-I1-S</i>	GCTCCAAAGGACTTGTACGTG	21
<i>Pd-I1-AS</i>	TGATCTGAAGGGCAGCATTTC	21
<i>Pd-I2-S</i>	CTGCCGATACTGAACCTGAGC	21
<i>Pd-I2-AS</i>	GCGGTCAAATCGCACTCC	19
<i>Lag3-S</i>	CTGGGACTGCTTTGGGAAG	19
<i>Lag3-AS</i>	GGTTGATGTTGCCAGATAACCC	22
<i>Tim3-S</i>	TCAGGTCTTACCCTCAACTGTG	22
<i>Tim3-AS</i>	GGCATTCTTACCAACCTCAAACA	23
<i><math>\beta</math>-Actin-S</i>	GGCTGTATTCCCCTCCATCG	20
<i><math>\beta</math>-Actin-AS</i>	CCAGTTGGTAACAATGCCATGT	22

## Supplementary Figures



**Figure S1. Pulmonary melanoma metastasis stimulates PD-1, PD-L2, LAG3 and TIM3.** 8-week-old WT mice were given B16-F10 (B16) melanoma cells or control vehicle (PBS) and the expression of immune checkpoint molecules was evaluated 2 weeks later. Real-time RT-PCR (RT-PCR) was used to quantitate the levels of mRNA encoding PD-1 (A), PD-L2 (B), LAG3 (C) and TIM3 (D) in the lungs from mice treated intravenously with PBS (B16 -) or B16 cells (B16 +). Each dot represents an evaluation in an individual animal. The plotted values represent the mean  $\pm$  SEM of the evaluations represented by the individual dots. \* $p < 0.05$ , \*\* $p < 0.01$  ( $t$ -test).

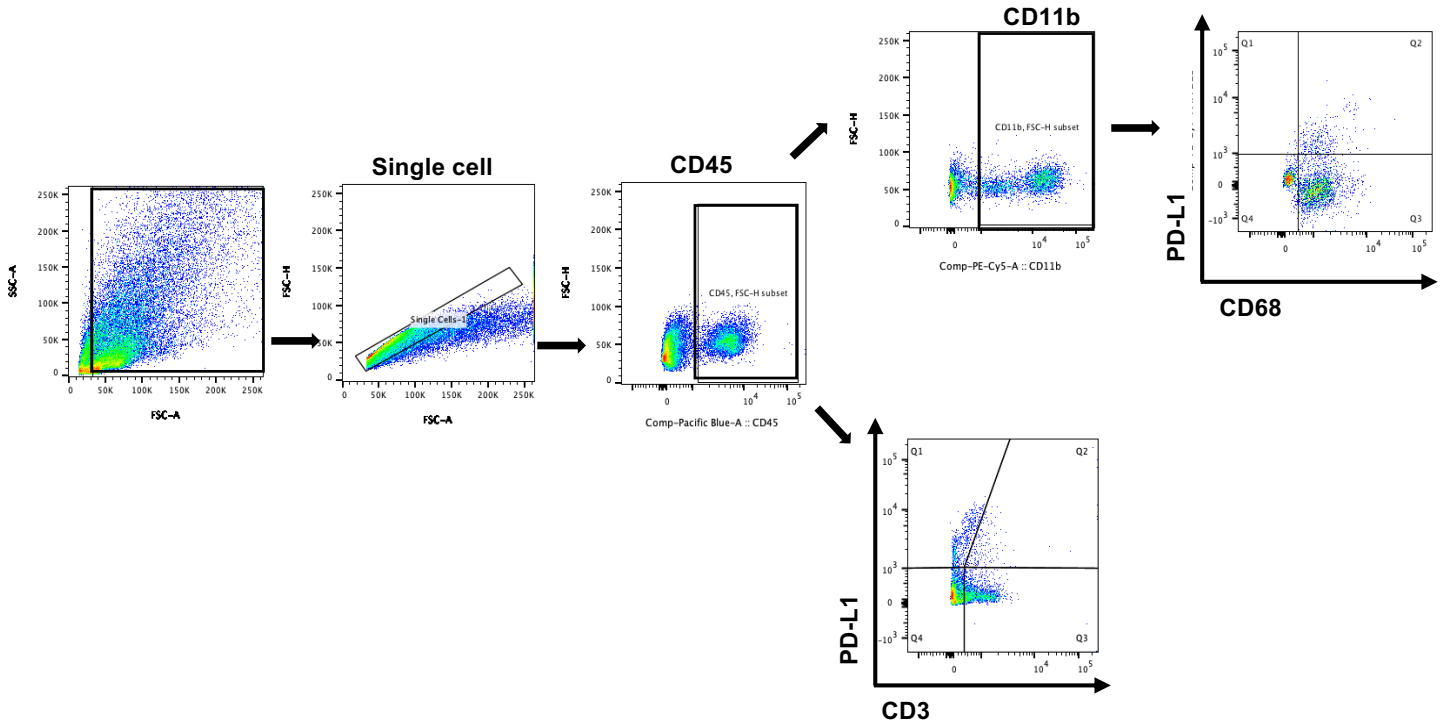


**Figure S2. Gating strategy of the FACS analysis used in the evaluation of macrophages and T cells in the lung of mice after melanoma cell challenge.** 8-week-old WT mice were challenged with vehicle (PBS) or B16-F10 melanoma cells, then the lungs were harvested on day 14 after melanoma cell injection and subjected to FACS evaluation. The inflammatory cells were first enriched with CD45 (+) then followed CD11b/CD68(+) for macrophages and CD3(+) T cells were subjected to the evaluation of PD-L1 expression.

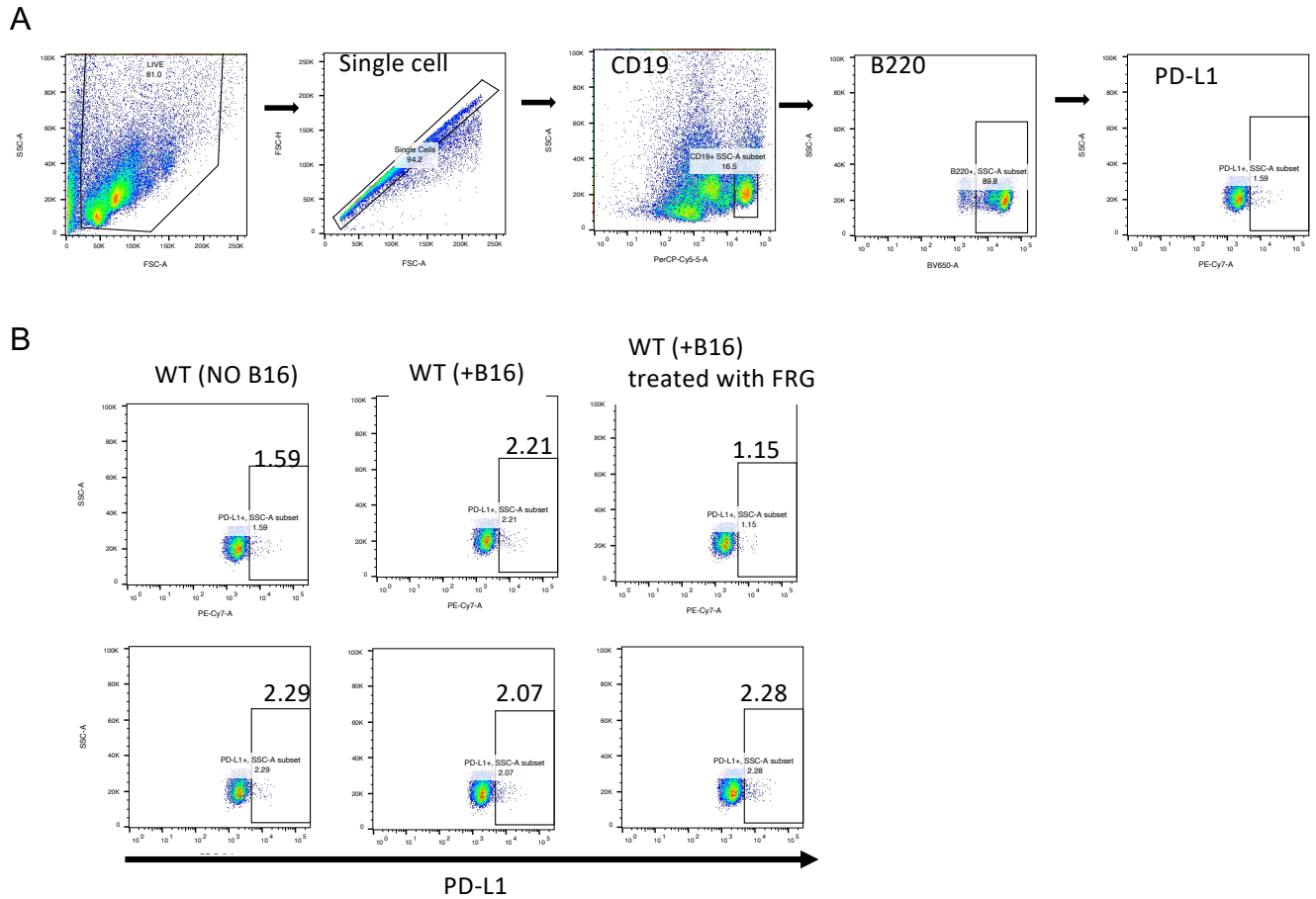


**Figure S3. PD-L1 expression in lung resident B cells with and without melanoma lung metastasis.** 8 weeks old WT mice were challenged with vehicle (PBS) or B16-F10 melanoma cells, then the lungs were harvested on day 14 after melanoma cell injection and subjected to FACS evaluation. (A) Gating strategy of lung resident B cells (CD19+/B220+) expressing PD-L1. (B) Representative FACS evaluations (two mice/group) on the PD-L1 expressing lung resident B cells.

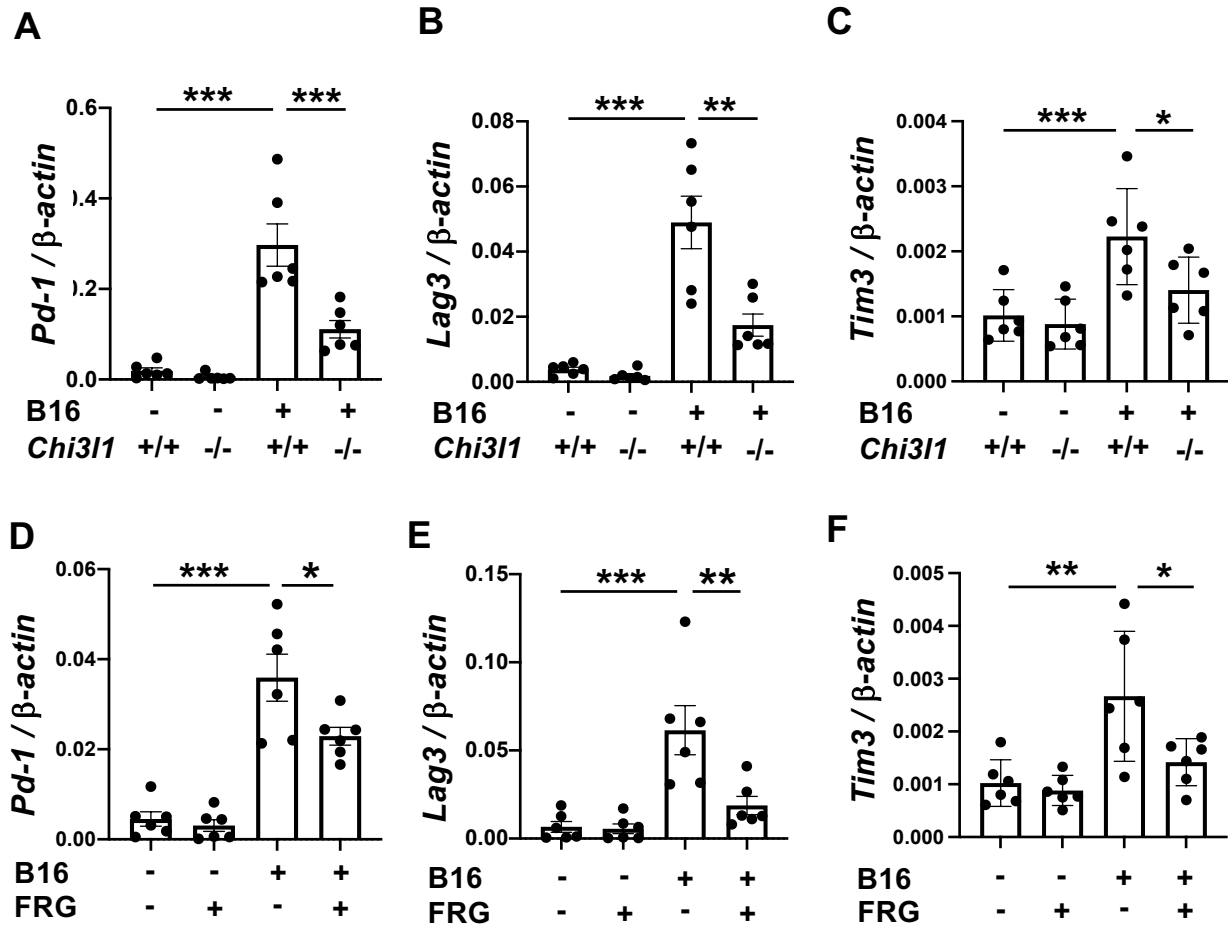


**Figure S4. Chi311 plays a critical role in B16 melanoma stimulation of pulmonary PD-1, LAG3 and TIM3.** 8-week-old WT (+/+) and Chi311 null (-/-) (*Chi311*<sup>-/-</sup>) mice were given B16 melanoma cells or vehicle control. They were then treated with an anti-Chi311 antibody (FRG) or isotype control antibodies and the expression of PD-1, LAG3 and TIM3 was evaluated 2 weeks later. (A-C) RT-PCR was used to quantitate the levels of mRNA encoding PD-1, LAG3 and TIM3 in the lungs from wild type (WT) (*Chi311* +/+) and Chi311 null (*Chi311* -/-) mice given PBS vehicle (B16 -) or B16 cells (B16 +). (D-F) RT-PCR evaluation of the levels of mRNA encoding PD-1, LAG-3 and TIM3 in the lungs from WT mice treated with PBS vehicle (B16 -) or B16 cells (B16 +) that were treated with FRG (FRG+) or vehicle (FRG-). Each dot represents the evaluation in an individual animal. The plotted values represent the mean  $\pm$  SEM of the noted evaluations represented by the individual dots. \**P*<0.05, \*\**P*<0.01, \*\*\**P*<0.001 (One-way ANOVA with Turkey post hoc test).

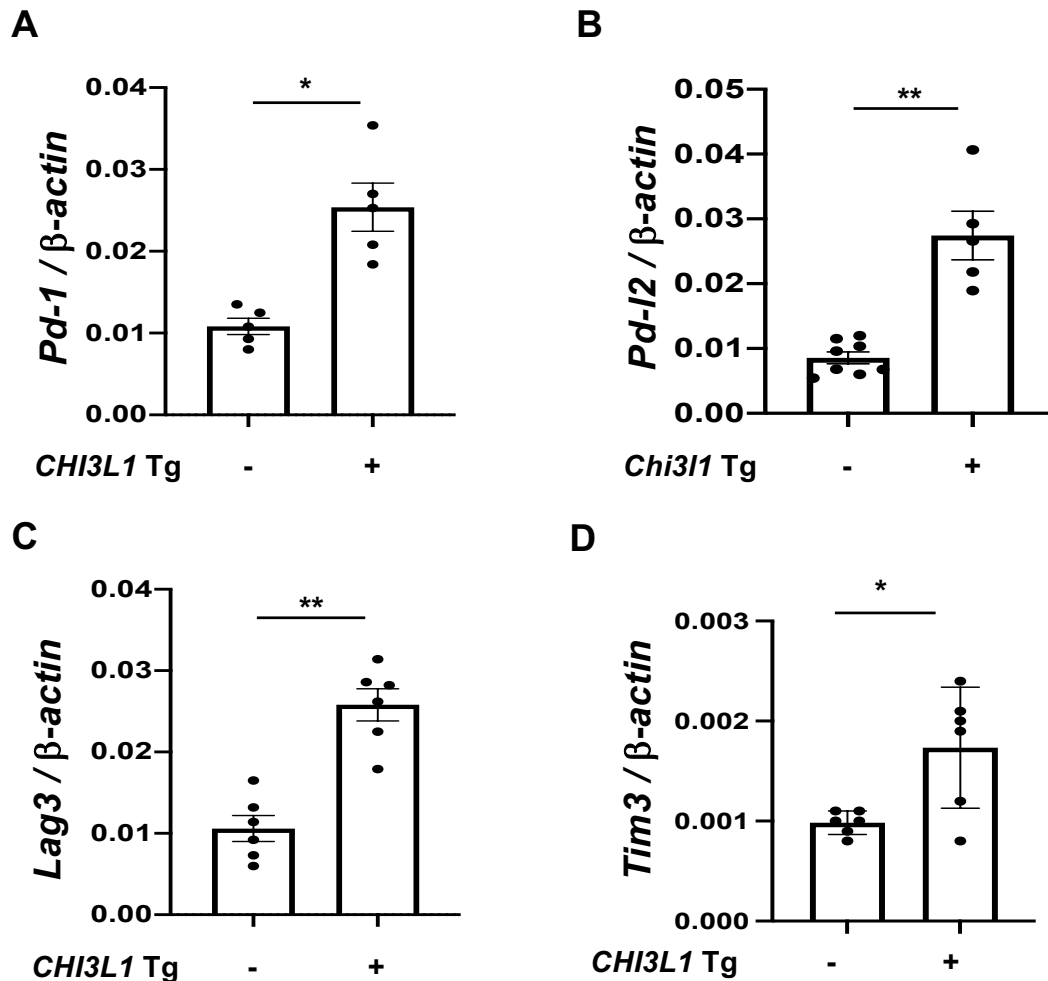


**Figure S5. Transgenic Chi3l1 stimulates PD-1, PD-L2, LAG3 and TIM3 in the normal lung.** 8-week-old WT (-), *CHI3L1* Tg (+) mice were used to evaluate the levels of mRNA encoding PD-1 (A), PD-L2 (B), LAG3 (C), and TIM3 (D) in the lung. RT-PCR was used to quantitate the levels of mRNA in the lungs from WT mice (*CHI3L1* Tg -) and mice in which *CHI3L1* was overexpressed in the lung in a transgenic manner (*CHI3L1* Tg +). Each dot represents the evaluation in an individual animal. The plotted values represent the mean  $\pm$  SEM of the noted evaluations represented by the individual dots. \* $p < 0.05$ , \*\* $p < 0.01$  (*t* test).

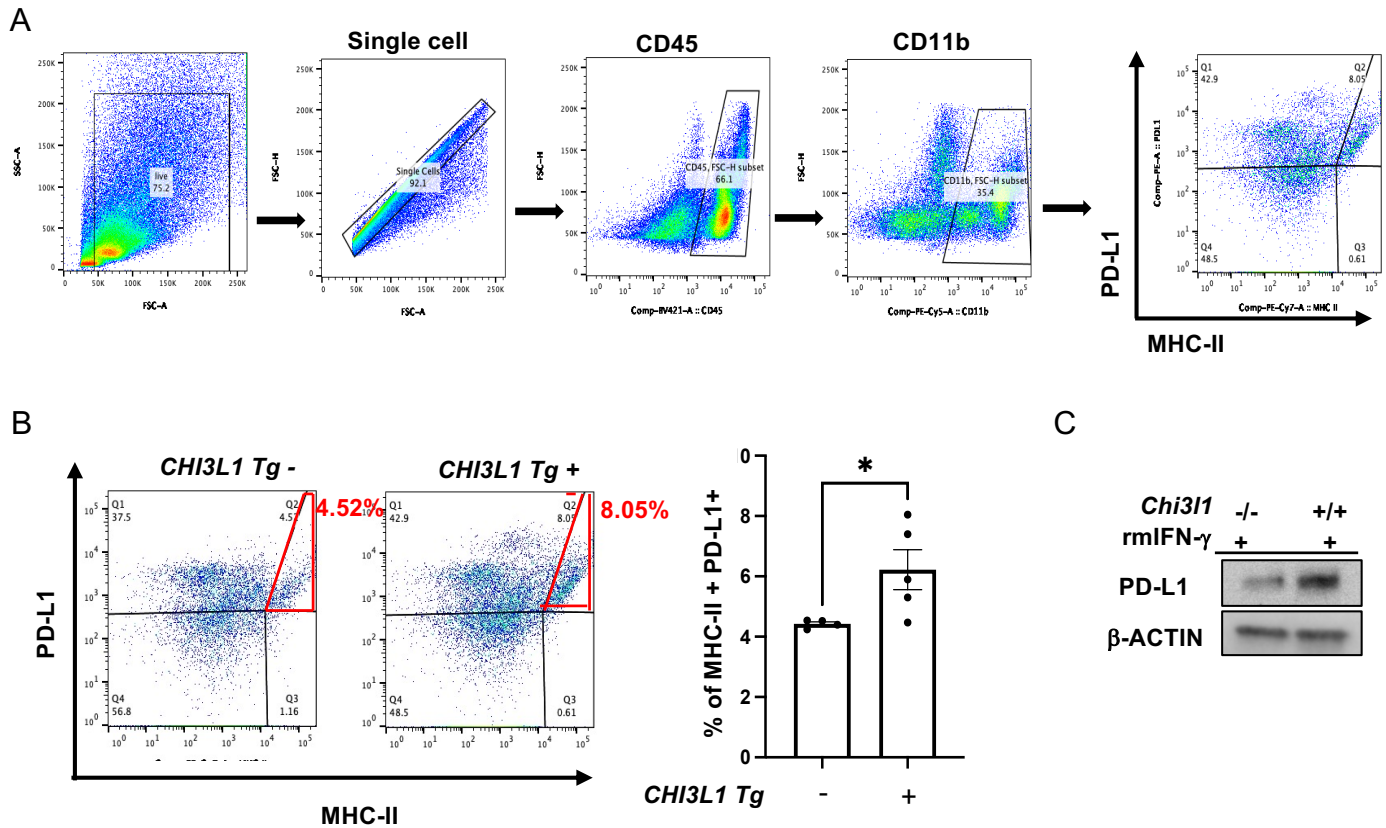


**Figure S6. Chi311 mediates rIFN- $\gamma$ -stimulated expression of PD-L1 in lung resident macrophages.** (A) Gating strategy used for the evaluation of PD-L1 in lung resident macrophages (CD45+/CD11b+)/MHCII(+)/PD-L1(+) cells). (B) FACS evaluations on PD-L1 expression in lung resident macrophages from WT (*CHI3L1*<sup>-</sup>) and CHI3L1 Tg mice. (C) Western blot evaluation to test the ability of rIFN- $\gamma$  to stimulate PD-L1 in lung resident macrophages from WT and *Chi311*<sup>-/-</sup> mice. The values in bar graph of panel B represent the mean $\pm$ SEM of the noted evaluations. \* $p < 0.05$  ( $t$  test).

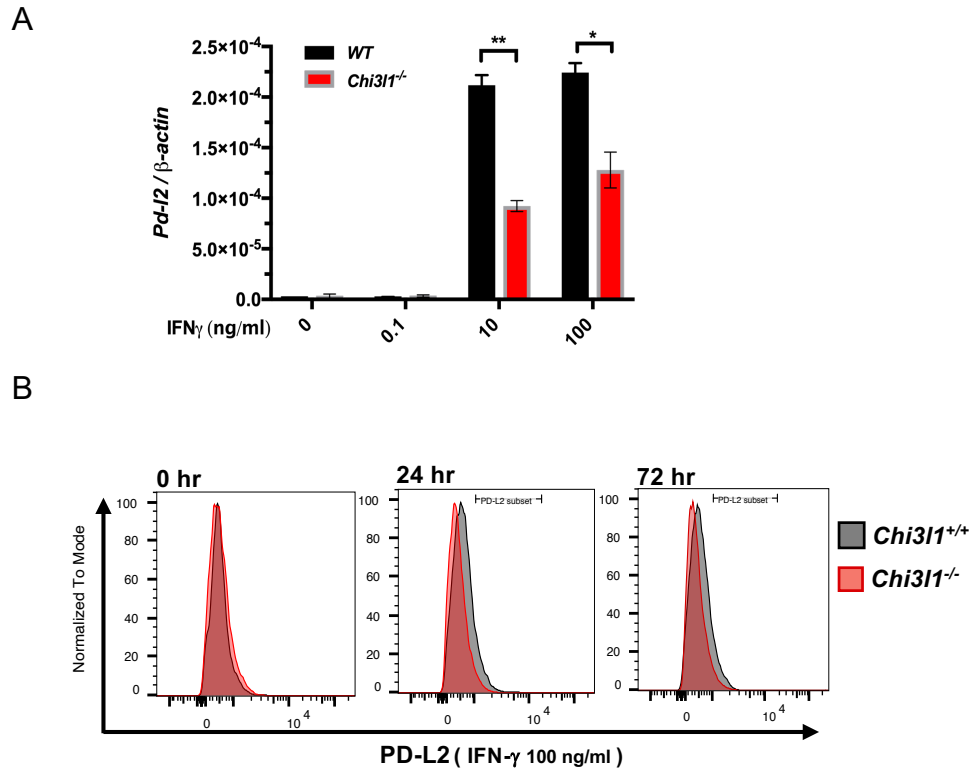


**Figure S7. IFN- $\gamma$ -stimulates macrophage PD-L2 via a Chi311-dependent mechanism.** Bone marrow derived macrophages (BMDM) prepared from 6-8 weeks old male WT and Chi311<sup>-/-</sup> mice and were used to evaluate the importance of Chi311 in rIFN- $\gamma$  stimulation of PD-L2. (A) rIFN- $\gamma$ -stimulation of PD-L2 mRNA expression in BMDM from WT and Chi311<sup>-/-</sup> mice. (B) FACS evaluations of the ability of rIFN- $\gamma$  to stimulate PD-L1 in BMDM prepared from WT and Chi311<sup>-/-</sup> mice. The values in panel A represent the mean $\pm$ SEM of the noted evaluations (n=5 mice/each). \*p<0.05, \*\*p<0.01 (*t* test). Panel B is a representative of a minimum of 2 separate evaluations.



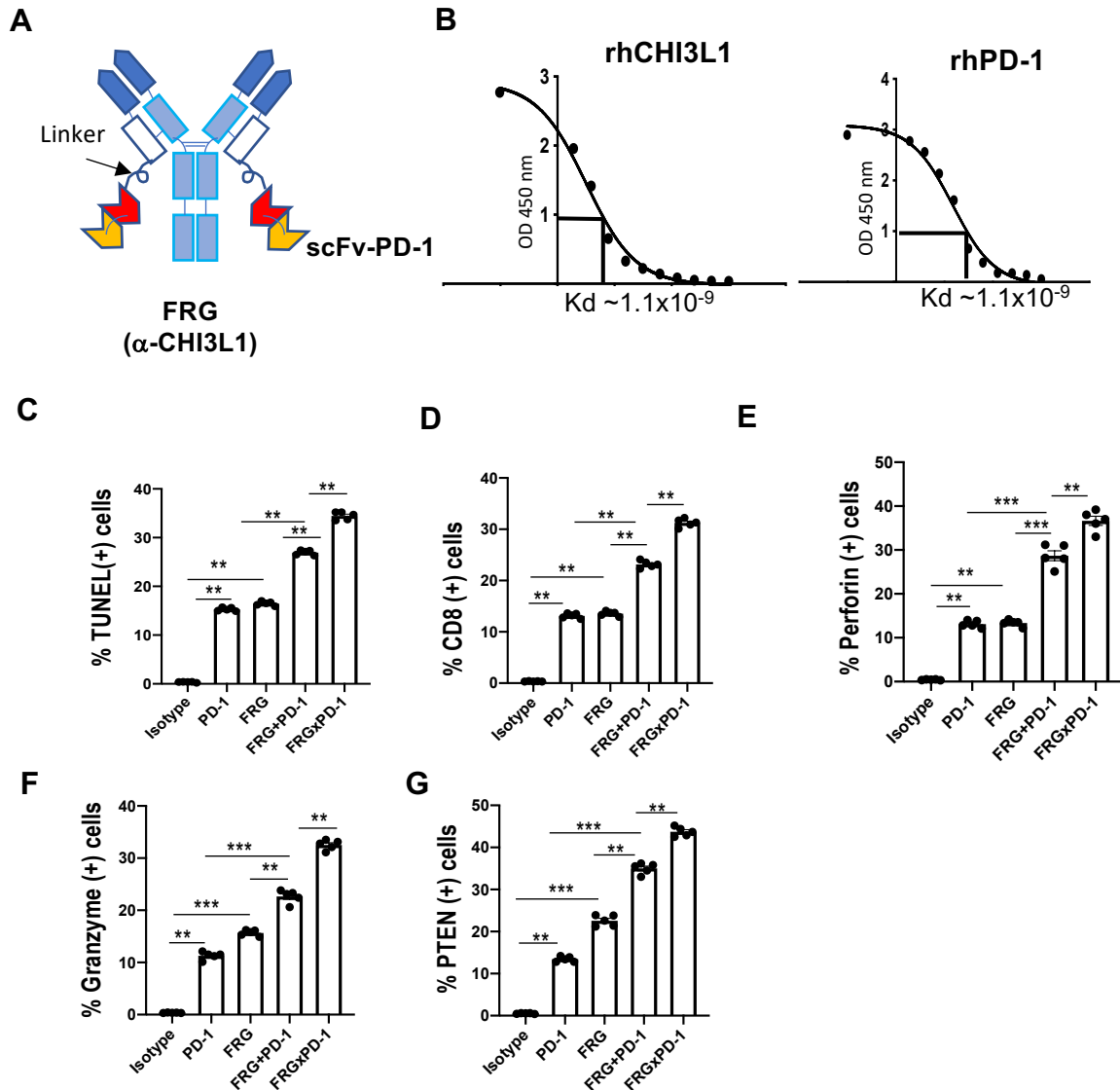


**Figure S8. The structure and the binding affinity of FRGxPD1 bispecific antibody and synergistic CTL-mediated tumor cell response and PTEN accumulation.** (A) Schematic illustration of the structure of the bispecific antibody FRGxPD-1 in which anti-PD-1 is linked to FRG via its light chain. (B) The affinity of FRGxPD1 antibody was evaluated by competitive ELISA against recombinant human (rh) CHI3L1 and rhPD-1. (C-G) Bispecific antibodies that simultaneously target Chi3l1 and PD-1 induce synergistic CTL-mediated tumor cell death responses and tumor cell PTEN accumulation. The antitumor effects of FRGxPD-1 bispecific antibody was tested in co-culture of system of Jurkat cells and B16-F10 murine melanoma cells as described in the Materials and Methods. (C) Quantitation of apoptotic tumor cell death using in situ cell death detection kit-fluorescein dUTP. (D-G) Quantification of T cell CD8<sup>+</sup> (D), perforin (E) and granzyme (F) accumulation. (G) quantification of tumor cell PTEN accumulation in co-cultures. These evaluations were undertaken using fluorescent microscopy (x20 of original magnification). In these quantifications, 10 randomly selected fields were evaluated. The values in these panels are the mean  $\pm$  SEM. \*\* $p < 0.01$ , \*\*\* $p < 0.001$  (One-way ANOVA with Turkey post hoc test).